

## Stability and the proximity theorem in Casimir actuated nano devices

R Esquivel-Sirvent<sup>1</sup>, L Reyes and J Bárcenas

Instituto de Física, UNAM, Apdo. Postal 20-364, México D F, México 01000

E-mail: [raul@fisica.unam.mx](mailto:raul@fisica.unam.mx)

*New Journal of Physics* **8** (2006) 241

Received 4 May 2006

Published 20 October 2006

Online at <http://www.njp.org/>

doi:10.1088/1367-2630/8/10/241

**Abstract.** A brief description of the stability problem in micro and nano electromechanical devices (MEMS/NEMS) actuated by Casimir forces is given. To enhance the stability, we propose the use of curved surfaces and recalculate the stability conditions by means of the proximity force approximation. The use of curved surfaces changes the bifurcation point, and the radius of curvature becomes a control parameter, allowing a rescaling of the elastic restitution constant and/or of the typical dimensions of the device.

### Contents

<b>1. Introduction</b>	<b>1</b>
<b>2. Basic zero-temperature calculations</b>	<b>3</b>
<b>3. Theoretical description of the pull-in dynamics</b>	<b>4</b>
<b>4. Curved surfaces in MEMS</b>	<b>5</b>
<b>5. Conclusions</b>	<b>8</b>
<b>Acknowledgments</b>	<b>8</b>
<b>References</b>	<b>8</b>

### 1. Introduction

The scaling down of many mechanical systems to the micro and nano scale, generically referred to as MEMS and NEMS, opens a new area of applications of the Casimir force. Since the

<sup>1</sup> Author to whom any correspondence should be addressed.

fundamentals of the Casimir force are well known, we will just remind the reader that Casimir's original result referred to the attraction between two neutral parallel plates made of a perfect conductor [1]. For arbitrary materials, Casimir's results were generalized by Lifshitz [2].

Although Casimir's original paper dates from 1948, the recent revival in the Casimir force is in part due to a series of precise experiments to measure this force using torsional balances [3], micro torsional balances [4]–[6] and atomic force microscopy [7] among other techniques [8]. All these experiments measure the deflection of a movable part in the presence of Casimir forces. Indeed, Chan *et al* [9] showed that Casimir forces can excite a micro torsional balance in their nonlinear mode. Thus, this apparently innocuous force is important in the design and operation of MEMS and NEMS. Experimentally, it will be of interest to measure the Casimir force at any separation between the plates or most commonly between a plate and a sphere. However, as the separation decreases, there is a critical separation at which the elements jump to contact and they adhere. Not only in Casimir force experiments, but in atomic force microscopy operations this pull-in is a well-known limitation when measuring forces as a function of distance [10, 11].

In general, the pull-in instability or jump to contact occurs when two components of the device adhere to each other due to the presence of an attractive force. This is a cause of failure of MEMS and NEMS. A micro or nano device has movable parts that are actuated by a force [12] and in their design there is an elastic restitutive force that brings the movable part to its original position. The most common examples are electrostatically driven devices [13]–[15], such as capacitive accelerometers or electrostatic micropumps. The basic model to study MEMS and NEMS is a spring mass model first worked by Nathanson *et al* [16]. Although a simple model, it reproduces all the main features of micro devices, to which an effective spring constant can be associated [17, 18]. For example, a cantilever with one fixed end and a load applied at the free end [19] has a spring constant  $\kappa \sim Ewt^3/l^3$ , where  $E$  is the Young's modulus,  $l$  the length,  $w$  its width and of thickness  $t$ . The basic spring model system typically used is shown in figure 1. Two plates of mass  $m$  one fixed and one attached to a linear spring of elastic constant  $\kappa$ . The plates attract to each other with a force that can be due to electrostatic interactions, Casimir forces or both. The formalism to describe the pull-in dynamics is presented in section 3.

The study of Casimir forces in MEMS goes back to the work of Serry *et al* [20, 21]. This particular study considered in an approximate way the role of finite conductivity and is the basis for the calculation we present in this paper. Since then, other authors made observations on the role that Casimir forces have in the pull-in and adhesion phenomena in MEMS [22]–[24]. The pull-in instability due to the Casimir force has been given consideration in many engineering works assuming the perfect conductor approximation [25]. Other theoretical descriptions that take into account the finite conductivity have also been considered recently [24, 26]. In this paper, we first give a short description of the problem of stability in MEMS and NEMS actuated by Casimir forces and propose a method to improve the stability using curved elements.

There are several important theoretical issues concerning the Casimir effect. In this paper, the calculations are done considering systems at zero temperature and assuming that the electromagnetic response of the materials is local. That is, any dielectric function we consider will depend on frequency only. The question of course, is the relevance of incorporating the effects of finite temperature and nonlocality. For MEMS and NEMS applications, given the typical separations involved in these devices, a zero temperature and local approach is justified: the corrections due to these effects are small at the typical separations at which MEMS and NEMS operate. Plenty of information on nonlocality and temperature effects can be found in

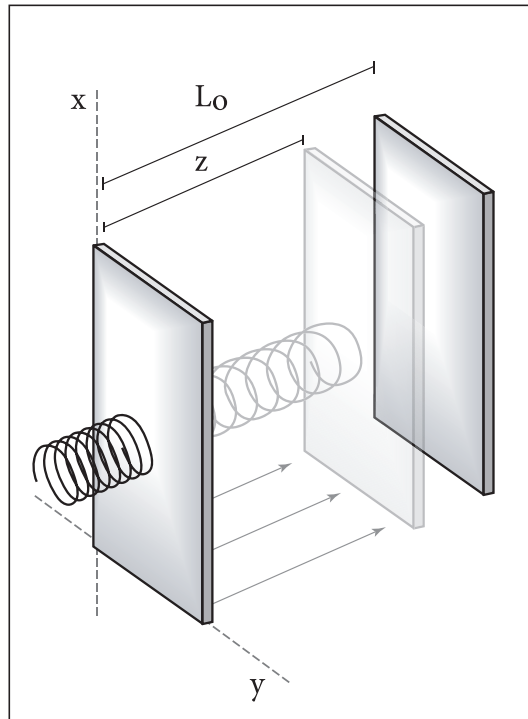


**Figure 1.** Geometry and coordinate system of the parallel plate configuration. The spring of elastic constant  $\kappa$  represents a restoring force in a MEMS/NEMS device.

[27]–[32]. Another effect that will be ignored is surface roughness. Its effect in micro devices has been studied by Palazantzas [33, 34].

## 2. Basic zero-temperature calculations

To set our notation and formulation, we briefly describe the usual Casimir force calculation via the Lifshitz formula [27]. For the canonical system depicted in figure 1, two parallel plates labelled  $i = 1, 2$  are characterized by their thickness  $d_i$  and dielectric function  $\epsilon_i(\omega)$ . The plates are separated a distance  $L = L_0 - z$ , in our coordinate system. Define the wave vector  $q = \omega/c = \sqrt{k^2 + Q^2}$ , where  $k$  is the wave vector component perpendicular to the surface and  $Q$  corresponds to the component parallel to the surface. The Lifshitz formula is given by [27]

$$F = \frac{\hbar c}{2\pi^2} \int_0^\infty Q \, dQ \int_{q>0} dk \frac{k^2}{q} (G^s + G^p), \quad (1)$$

where  $G_s = (r_{1s}^{-1} r_{2s}^{-1} \exp(2ikL) - 1)^{-1}$  and  $G_p = (r_{1p}^{-1} r_{2p}^{-1} \exp(2ikL) - 1)^{-1}$ . In these expressions, the factors  $r_{p,s}$  are the reflectivities for either  $p$  or  $s$  polarized light. When the reflectivities are replaced by the Fresnel coefficients, the original Lifshitz formula for half-spaces is recovered. Casimir's result for ideal conductors is obtained when  $|r_p| = |r_s| = 1$  for both plates, this is

$$F = -\frac{\hbar c \pi^2}{240L^4}. \quad (2)$$

The Lifshitz formula written in terms of the reflection amplitudes can be applied to a broad variety of systems such as composites or layered media [35]–[37], provided the reflectivities can be measured or calculated as a function of frequency.

### 3. Theoretical description of the pull-in dynamics

The description of pull-in in simple mass-spring models is well established [13]. In this section, we present only the main results. The pull-in occurs when the attractive force overcomes the elastic force and no steady state positions of the movable plate exist. To be more specific, let the actuating force that depends on the separation of the plates be of the form  $f(L_0 - z) = \alpha/(L_0 - z)^n$  with  $n$  a positive integer and  $\alpha$  a constant. The equation of motion of the plate is

$$-\kappa z + f(L_0 - z) = m \frac{d^2 z}{dt^2} \quad (3)$$

The previous equation can be written as

$$-v + \frac{\lambda}{(1-v)^n} = \frac{d^2 v}{d\tau^2}, \quad (4)$$

where the normalized quantities  $v = z/L_0$  and  $\tau = t\sqrt{\kappa/m}$  have been used, and the parameter  $\lambda$  is defined as

$$\lambda = \alpha/(\kappa L_0 L_0^n). \quad (5)$$

is a bifurcation parameter that physically represents the ratio of the minimum value of the actuating force when there is no deflection of the spring to the maximum possible elastic force when the plates are in contact.

Depending on the values of  $\lambda$ , there are several possible solutions of equation (4). The plate will oscillate, will reach a steady state or will collapse into the second plate when there are no steady state solutions of equation (4) possible. For the Casimir force case, this is clearly shown in the energy curves for different values of  $\lambda$  in the paper by Serry *et al* [20]. We are interested in the values of  $\lambda$  for which no steady states exist.

Setting the left-hand side of equation (4) equal to zero, we can solve for the parameter  $\lambda$  as

$$\lambda = v(1-v)^n. \quad (6)$$

The plot of equation (6) gives the bifurcation diagram, as shown in figure 2 for different values of  $n$ . As  $\lambda$  increases the separation between the plates decreases, recalling that  $v = 1$  means that the plates are in contact, until there is a fold at a value of  $\lambda = \lambda_p$ . All the points of the lower branch represent the equilibrium position reached by the moving plate for a particular value of  $\lambda$ . At  $\lambda_p$  the pull-in occurs the moving plate is at a position  $v_p$ . At any point in the upper branch the plates jump to contact. For example, take the curve for  $n = 4$ . At  $\lambda = 0.04$ , there are two possible values of  $v$ . In the lower branch  $v = 0.04$  and it is a steady state solution. At this point, the elastic force equals the attractive force. For the upper branch, we have a value of  $v = 0.46$ . At this position, the plate jumps to contact. From figure 2, we see that the bifurcation

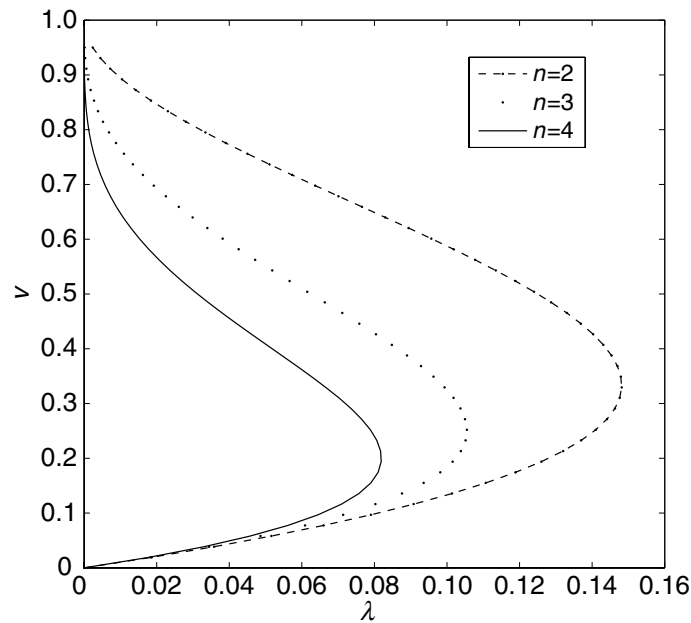


**Figure 2.** Bifurcation diagram for a simple-lumped one degree of freedom system for several values of  $n$ , assuming the actuating force goes as approximately  $1/(1-v)^n$ .

curves change with the value of  $n$  and the fold is at  $(v_p, \lambda_p) = (1/(n+1), \lambda_p)$ . Changing the bifurcation diagram, allows a wider range of steady state positions. Take for example the value of  $v = 0.22$ . For  $n = 4$ , the plates will collapse. However, this same value of  $v$  is in a steady state position for the curves  $n = 2, 3$ . Thus, the travel range of the moving plate is extended. From the definition of  $\lambda$ , we see that it is inversely proportional to the spring constant. Extending the possible values of  $\lambda$  for which we have steady states can allow a reduction in the spring constant in a given experiment.

#### 4. Curved surfaces in MEMS

In this section, we study the effect of introducing curved surfaces in the simple mass-spring system as shown in figure 3, when the device is actuated by a Casimir force. From the practical point of view, one problem is to extend the travel range of the moving plate beyond  $v_p$  for a particular value of  $\lambda$ . While for an electrostatically actuated device there have been some attempts to do this [38], the case of Casimir actuated MEMS/NEMS has received little attention. Although one can select the parameters of the system so as to avoid the pull-in, in many applications this can be difficult to achieve, as in the case of Casimir force experiments. The distance between the sphere and plane are fixed and the force is determined by measuring the deflection of the plate. The distance is reduced, and the measurement repeated. Eventually a separation  $L_0$  is reached such that for the corresponding value of  $\lambda$  the system collapses. The softer the spring constant, the deflection of a cantilever or torsional balances can be measured more precisely. The caveat is that it is not possible to make measurements at small separations without the jump-to-contact. Previously [26], we showed that one way of changing the bifurcation point is working with

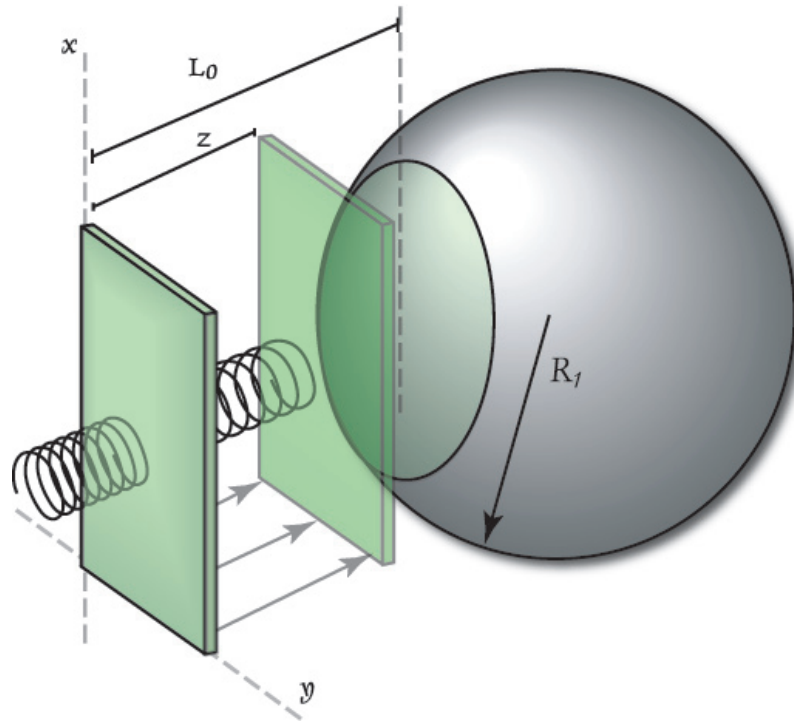


**Figure 3.** The simple-lumped system representing the plate–sphere geometry used in our calculation of stability.

different materials. The value of  $\lambda_p$  changes with the plasma frequency of different metals, assuming they are described by a Drude-like dielectric function, the damping parameter plays a minor role in the overall behaviour of the system. For poor conductors, the strength of the Casimir force is smaller and the system is less prompt to jump-to-contact for a given value of  $\lambda$ .

Now we consider the effect of curvature. This can be done using the proximity theorem, or proximity force approximation (PFA) that has been used in most experimental set-ups [5]–[7]. The PFA states that the force between two curved surfaces of radius of curvature  $R_1$  and  $R_2$  is proportional to the free energy between the parallel plates, being the constant of proportionality  $\pi$  times the harmonic mean of the radii of curvature [39, 40].

Without loss of generality consider again the type of force used in equation (4). This force is derived from a free energy  $f = -\partial\mathcal{E}/\partial z$ , where

$$\mathcal{E} = \frac{\alpha}{1-n} \frac{1}{(L_0 - z)^{n-1}}. \quad (7)$$

Thus, the force between a plane and a sphere according to the PFA is

$$F = 2\pi R \frac{\alpha}{1-n} \frac{1}{(L_0 - z)^{n-1}}. \quad (8)$$

The equilibrium equation now takes the form

$$\frac{R\hbar c\pi^3}{360\kappa L_0^4} = (1-v)^3 v \quad (9)$$

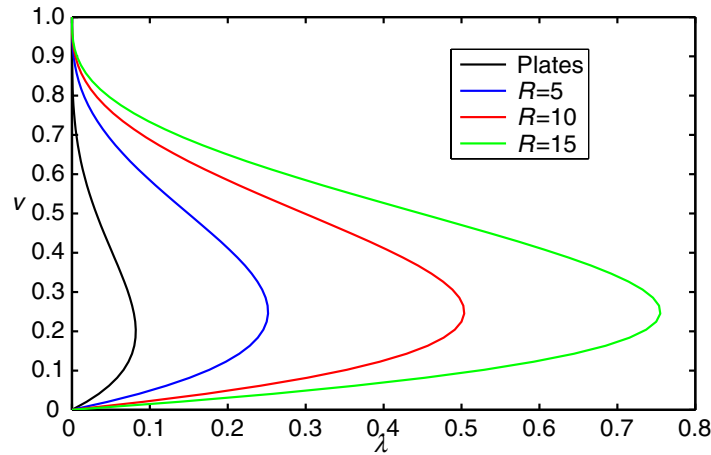


**Figure 4.** Bifurcation diagram for the plate–sphere system for different values of  $\bar{R}$ . For comparison, the bifurcation curve for the parallel plate configuration is also included.

where we have used equation (8) with  $\alpha = A\hbar c\pi^2/240$ . Since we want to compare with the parallel plate case, we introduce the definition of  $\lambda$  given by equation (5), and the equilibrium equation becomes

$$\lambda = \frac{3A}{2\pi RL_0}(1-v)^3v. \quad (10)$$

If the area of the plate is of the order of  $R^2$ , we finally have

$$\lambda = \frac{3\bar{R}}{2\pi}(1-v)^3v, \quad (11)$$

where  $\bar{R} = R/L_0$ . In figure 4, we show the bifurcation diagram again for the parallel plates and for the sphere–plate system for different values of  $\bar{R}$ . The bifurcation point  $\lambda_p$  is shifted just by increasing the radius. The pull-in point of equation (11) is  $v = 1/4$ ; this corresponds to a maximum value of

$$\lambda_p = \frac{81}{512\pi}\bar{R}. \quad (12)$$

Indirectly, proximity allows us to vary the magnitude of the force, by means of geometry without having to change the materials. As in figure 2, what can be achieved is to extend the range of possible values of  $\lambda$  for which steady state solutions exists. In this example, we considered the plate–sphere problem but the results hold if we had two curved surface. In this case, the radius  $R$  in equation (8) is the harmonic mean of the radii of curvature of the two surfaces. Then we have two control parameters  $R_1$  and  $R_2$ .

## 5. Conclusions

In this study, we give a brief introduction to the problem of MEMS and NEMS actuated by Casimir forces, with particular emphasis on the problem of the pull-in instability. To control this instability, we consider the use of curved surfaces, calculating the force by means of the proximity force approximation. The only caveat is that the PFA can be applied only if the radius of curvature is larger than the plate–sphere separation. This approach introduces the radius of the sphere as a control parameter. In this study, we were interested in the effect of using curved surfaces and assumed in the calculations perfect conductivity of the materials. However, the dielectric properties can be incorporated in the calculations and effectively constitute another control parameter for the stability of the system.

## Acknowledgments

Partial support from CONACyT-Mexico grant 44306 and DGAPA-UNAM IN-101605. We thank Jordan Maclay for his careful reading of the manuscript and comments.

## References

- [1] Casimir H B G 1948 *Proc. K. Ned. Akad. Wet.* **51** 793
- [2] Lifshitz E M 1956 *Sov. Phys.—JETP* **2** 73
- [3] Lamoreaux S K 1998 *Phys. Rev. Lett.* **78** 5  
Lamoreaux S K 1998 *Phys. Rev. Lett.* **81** 5475
- [4] Chan H B, Aksyuk V A, Kleiman R N, Bishop D J and Capasso F 2001 *Science* **291** 1941  
Chan H B, Aksyuk V A, Kleiman R N, Bishop D J and Capasso F 2001 *Phys. Rev. Lett.* **87** 211801
- [5] Iannuzzi D, Lisanti M and Capasso F 2004 *Proc. Natl Acad. Sci. USA* **101** 4019
- [6] Decca R S, López D, Fischbach E and Krause D E 2003 *Phys. Rev. Lett.* **91** 050402
- [7] Mohideen U and Roy A 1998 *Phys. Rev. Lett.* **81** 4549
- [8] Bressi G, Carugno G, Onofrio R and Ruoso G 2002 *Phys. Rev. Lett.* **88** 041804
- [9] Chan H B, Aksyuk V A, Kleiman R N, Bishop D J and Capasso F 2001 *Phys. Rev. Lett.* **87** 211801
- [10] Gady B, Schlee D, Reifenberger R and Rimai D S 1998 *J. Adhesion* **67** 291
- [11] Hays D A 1995 *Fundamentals of Adhesion and Interfaces* vol 61, ed D S Rimai, L P DeMejo and K L Mittal (Utrecht: VSP)
- [12] Ekinci K L and Roukes M L 2005 *Rev. Sci. Instrum.* **76** 061101
- [13] Pelesko J A and Bernstein D H 2003 *Modeling MEMS and NEMS* (Boca Raton, FL: Chapman and Hall/CRC Press)
- [14] Pelesko J A 2002 *SIAM J. Appl. Math.* **62** 888
- [15] Flores G, Mercado G A and Pelesko J A 2003 *Proc. IDETC/CIE, 19th ASME Biennial Conf. on Mechanical Vibrations and Noise* (New York: ASME) pp 1–8
- [16] Nathanson H C, Newell W E, Wickstrom R A and Davis J R 1967 *IEEE Trans. Electron Devices* **14** 117
- [17] Nemirovsky Y 2001 *J. Microelectrom. Sys.* **10** 601
- [18] Lin W H and Zhao Y P 2005 *Microsyst. Technol.* **11** 80
- [19] Iannuzzi D, Deladi S, Gadgil V J, Sanders R G P, Schreuders H and Elwenspoek M C 2006 *Appl. Phys. Lett.* **88** 053501
- [20] Serry F M, Walliser D and Maclay G J 1995 *IEEE J. Microelectromech. Sys.* **4** 193
- [21] Serry F M, Walliser D and Maclay G J 1998 *J. Appl. Phys.* **84** 2501
- [22] Buks E and Roukes M L 2001 *Europhys. Lett.* **54** 220
- [23] Buks E and Roukes M L 2001 *Phys. Rev. B* **63** 033402



- [24] Chumak A A, Milonni P W and Berman G P 2004 *Phys. Rev. B* **70** 085407
- [25] Zhao Y P, Wang L S and Yu T X 2003 *J. Adhesion Sci. Technol.* **17** 519
- [26] Barcenas J, Reyes L and Esquivel-Sirvent R 2005 *Appl. Phys. Lett.* **87** 263106
- [27] Esquivel-Sirvent R, Villarreal C and Mochán W L 2003 *Phys. Rev. A* **68** 052104
- [28] Esquivel-Sirvent R and Svetovoy V 2004 *Phys. Rev. A* **69** 062102
- [29] Esquivel-Sirvent R and Svetovoy V 2005 *Phys. Rev. B* **72** 045443  
Svetovoy V and Esquivel-Sirvent R 2005 *Phys. Rev. E* **72** 036113
- [30] Lamoreaux S K 2005 *Rep. Prog. Phys.* **68** 201
- [31] Bordag M, Mohideen U and Mostepanenko V M 2001 *Phys. Rep.* **353** 1–205
- [32] Milton K A 2004 *J. Phys. A: Math. Gen.* **37** R209
- [33] Palazantzas G 2005 *J. Appl. Phys.* **97** 126104
- [34] Palazantzas G 2005 *J. Appl. Phys.* **98** 034505
- [35] Esquivel-Sirvent R, Villarreal C and Noguez C 2002 *Mat. Res. Symp. Proc.* **703** V3.3.1
- [36] Reyes L, Bárcenas J and Esquivel-Sirvent R 2005 *Phys. Status Solidi c* **2** 3059
- [37] Esquivel-Sirvent R, Villarreal C and Coccoletzi G H 2001 *Phys. Rev. A* **64** 052108
- [38] Hung E S and Senturia S D 1999 *J. Microelectron. Sys.* **8** 497
- [39] White L R 1983 *J. Coll. Sci. Int.* **95** 286
- [40] Blocki J, Randrup J, Swiatecki W J and Tsang C F 1977 *Ann. Phys.* **105** 463